



12 **Abstract**

13 The observed imbalance between the unsustainable consumption of available natural  
14 metal resources and finite deposits makes the recovery and recycling of metals from  
15 metal-containing wastes an imperative. Here, ionic-liquid-based aqueous biphasic  
16 systems (IL-based ABS) are proposed as an efficient alternative for selective metal  
17 recovery from real copper acid mine drainage (AMD) effluents. ABS composed of  
18 different IL and Na<sub>2</sub>SO<sub>4</sub> were evaluated for Zn, Al, Cu, Co and Ni extraction from both  
19 model solutions and AMD samples. It is shown that IL composed of thiocyanate anion  
20 ([SCN]<sup>-</sup>) presented a remarkable ability to extract metals from AMD through the  
21 formation of stable metal-complexes. The addition of NaSCN to ABS composed of  
22 tetrabutylammonium chloride ([N<sub>4444</sub>]Cl) allowed to mimic the use of [SCN]<sup>-</sup>-based IL  
23 with additional advantages: tunable metal selectivity by the concentration of [SCN]<sup>-</sup>  
24 added to the ABS, and reduction of system cost and environmental impact. Furthermore,  
25 at the [SCN]<sup>-</sup> concentration range studied here, it is observed the formation of a  
26 hydrophobic salt composed of IL cations and metal complex anions, which allows the  
27 selective extraction and recovery of transition metals in a single-step. The IL-rich phase  
28 recyclability in three extraction cycles is demonstrated, showing the possibility to recover  
29 two times more Zn than with a single extraction cycle while using the same amount of IL  
30 and thiocyanate. Salt-rich phases were also recycled in a new IL-based ABS for the  
31 subsequent Cu extraction and recovery. These results allow the development of a  
32 sustainable process for the selective sequential recovery of transition metals from AMD.

33

34 **Keywords:** waste valorization, recovery, liquid-liquid extraction, ionic liquids, process  
35 design.

36

## 37 **Introduction**

38 The growth of the world's population is creating a huge pressure on natural resources.  
39 The increased global demand for these raw materials is leading to metals scarcity and  
40 creating an unsustainable imbalance between supply and demand.<sup>1,2</sup> The reduced  
41 availability of minable deposits and their concentration in a limited number of countries  
42 will cause an increase of metals price and potential political instability.

43 Metal-containing wastes appear as an important secondary source of these raw materials  
44 and several efforts have been done to find novel and more efficient strategies for metals  
45 recovery and recycling. Mining industry residues are considered potential sources of  
46 valuable metals. This type of residues is produced in large amounts – about 20 to 25  
47 billion tons/year worldwide – and present high environmental impact if not correctly  
48 treated.<sup>3</sup> Acid mine drainage (AMD) are produced by mining activity, during and even  
49 after the end of mining exploitation. These are highly acidic waters that result from the  
50 oxidation of exposed sulfide-rich minerals, such as pyrite, pyrrhotite and arsenopyrite, by  
51 air and water.<sup>4</sup> Besides their high acidity and sulfate content, AMD also contain an  
52 important amount of dissolved elements and toxic metals, such as Fe, Al, Mn, Cu, Ni, Co,  
53 Pb, and As, whose composition is dependent on the ore body being explored. Due to the  
54 long-term environmental impact caused by these waters, the treatment and management  
55 of AMD is nowadays one of the biggest economic and environmental challenges faced  
56 by the mining industry.<sup>5,6</sup>

57 Metal recovery allows to add value to waste treatment processes; still only few works  
58 discuss the use of AMD as a potential secondary source of strategic metals.<sup>4,7-13</sup> Different  
59 technologies were developed, namely the application of fractional precipitation,<sup>8-10</sup>  
60 magnetic nanoparticles,<sup>11</sup> extraction resins<sup>12</sup> and remediation systems,<sup>13</sup> to recover  
61 transition metals and rare earth elements (REE). Amongst these, fractional precipitation  
62 is the technology that attracted most attention. This process is commonly used to treat  
63 AMD, is cost effective and can be easily applied at large scale. Furthermore, it was  
64 demonstrated by Yan et al.<sup>9</sup> through a simplified economic analysis, that when fractional  
65 precipitation is used to recover Fe, Cu, Zn and Mn present in AMD, the benefit obtained  
66 from the recycled metals is able to cover at least the costs of the chemical reagents used.  
67 However, this process results in the production of large amounts of sludges and metals  
68 recovery is hard to achieve. Similarly, the remaining proposed technologies also present  
69 some drawbacks, namely related with recovery efficiencies, associated costs, or low  
70 potential for scale-up.

71 Liquid-liquid extraction processes are commonly used at industrial level in the selective  
72 extraction and recovery of metals. Liquid-liquid systems are usually prepared by using  
73 volatile organic compounds, which are well known for their toxicity. Hydrophobic ionic  
74 liquids (IL) were proposed as an alternative due to their negligible vapor pressure and  
75 higher extraction efficiencies. However, IL composition based on fluorinated anions  
76 and/or long alkyl chains, which result in high viscosity, cost and environmental impact,  
77 limit their applicability.<sup>14</sup> Aqueous biphasic systems (ABS) composed of hydrophilic IL  
78 are more benign alternatives.<sup>15</sup> ABS are formed by the mixture of two water soluble  
79 solutes, namely salts and/or polymers, which above a certain concentration induces the  
80 formation of two immiscible aqueous phases.<sup>16,17</sup> IL-based ABS present a number of  
81 advantages derived from IL properties and their successful application to extract and  
82 separate metals was previously demonstrated.<sup>15,18–20</sup> However, the application of these  
83 systems to selectively recover metals from AMD as well as the stability of most IL-based  
84 ABS under acidic conditions was never evaluated.

85 A novel strategy for the sequential selective recovery of strategic metals from AMD  
86 water, collected from the Portuguese mine of São Domingos, using IL-based ABS is  
87 developed and presented in this work. São Domingos mine is in the Iberian Pyrite belt  
88 and was exploited during 100 years for pyrite, copper and sulfur production. During this  
89 time and even after its exhaustion, the exposure of the open pit mine to the atmospheric  
90 conditions resulted in the formation of AMD creating several environmental issues in this  
91 region.<sup>21</sup>

## 92 Methodology

93 A detailed description of the materials and methods used in this work is described in the  
94 **Supplementary Information (SI)**. AMD sample was collected in the open pit  
95 impoundment of the mine of São Domingos, Portugal. Sodium sulphate, Na<sub>2</sub>SO<sub>4</sub>,  
96 supplied by Merck with a purity of > 99 wt % was used in ABS formation mixed with  
97 ILs reported in **Table 1**. IL chemical structures are presented in **Figure S1** of the **SI**.

98  
99 **Table 1.** Name, acronym, purity (wt %) and supplier of the IL studied.

	IL	Acronym	Purity (wt %)	Supplier
(i)	1-butyl-3-methylimidazolium thiocyanate	[C <sub>4</sub> C <sub>1</sub> im][SCN]	> 98	Iolitec
(ii)	1-butyl-3-methylimidazolium dicyanamide	[C <sub>4</sub> C <sub>1</sub> im][N(CN) <sub>2</sub> ]	98	Iolitec
(iii)	1-butyl-3-methylimidazolium octylsulfate	[C <sub>4</sub> C <sub>1</sub> im][C <sub>8</sub> SO <sub>4</sub> ]	99	TermoFisher
(iv)	1-butyl-3-methylimidazolium triflate	[C <sub>4</sub> C <sub>1</sub> im][CF <sub>3</sub> SO <sub>3</sub> ]	99	Iolitec
(v)	1-butyl-3-methylimidazolium ethylsulfate	[C <sub>4</sub> C <sub>1</sub> im][C <sub>2</sub> SO <sub>4</sub> ]	98	Iolitec
(vi)	1-butyl-3-methylimidazolium tosylate	[C <sub>4</sub> C <sub>1</sub> im][TOS]	99	Iolitec
(vii)	1-butyl-3-methylimidazolium bromide	[C <sub>4</sub> C <sub>1</sub> im]Br	> 98	Iolitec
(viii)	1-heptyl-3-methylimidazolium chloride	[C <sub>7</sub> C <sub>1</sub> im]Cl	> 98	Iolitec
(ix)	1-dodecyl-3-methylimidazolium chloride	[C <sub>12</sub> C <sub>1</sub> im]Cl	> 98	Iolitec
(x)	tributylethylphosphonium diethylphosphate	[P <sub>4442</sub> ][DEP]	99	Cytec Ind.
(xi)	tributylmethylphosphonium methylsulfate	[P <sub>4441</sub> ][C <sub>1</sub> SO <sub>4</sub> ]	<i>pure</i>	Cytec Ind.
(xii)	tributyltetradecylphosphonium hydrogensulfate	[P <sub>44414</sub> ][HSO <sub>4</sub> ]	> 95	Iolitec
(xiii)	triisobutyl(methyl)phosphonium tosylate	[P <sub>1(444)1</sub> ][TOS]	<i>pure</i>	Cytec Ind.
(xiv)	bis(2-hydroxyethyl)dimethylammonium chloride	[N <sub>11(2OH)(2OH)</sub> ]Cl	99	Acros Organics
(xv)	benzyltributylammonium chloride	[N <sub>444Bz</sub> ]Cl	> 97	Acros Organics
(xvi)	tetrabutylammonium chloride	[N <sub>4444</sub> ]Cl	> 97	Sigma-Aldrich

100

### 101 Characterization of AMD from São Domingos

102 The nature and concentration of metals present in the AMD water sample from the mine  
103 of São Domingos were determined by inductively coupled plasma mass spectrometry  
104 (ICP-MS) using an Agilent Technologies 7700 Series spectrometer. The concentration of  
105 sulfates (SO<sub>4</sub>) was determined by ion chromatography using a Dionex 2000i equipment,  
106 while water pH and conductivity were measured at (25 ± 1) °C using a Mettler Toledo  
107 SevenMulti pH meter within ± 0.02. Details on AMD pre-treatment carried-out before  
108 metal extraction are presented in **SI**.

109

### 110 Metal extraction in IL-based ABS

111 Metals extraction was carried-out in ternary systems composed of 25 wt % of IL + 10  
112 wt % of Na<sub>2</sub>SO<sub>4</sub> + 65 wt % of H<sub>2</sub>O (metal standard aqueous solution or AMD sample).

113 Ternary mixtures composition was defined by comparing the binodal curves of previously  
114 reported phase diagrams for IL + Na<sub>2</sub>SO<sub>4</sub> ABS and choosing a mixture point common to  
115 all the biphasic regions (*cf.* **Table S1**).<sup>22</sup>

116 A first screening on IL-based ABS ability to extract metals was carried-out by using  
117 individual aqueous metal solutions of Cu, Ni and Co at 0.01 M. The ternary mixtures  
118 were vigorously stirred and, to guarantee the complete separation of the ABS coexisting  
119 phases and metals partition, the systems were centrifuged at (298 ± 1) K, for 30 min at  
120 3500 rpm. After this, the top and bottom phases were carefully separated, and their weight  
121 (within ± 10<sup>-4</sup> g) and volume (± 0.01 mL) were measured. The quantification of the metals  
122 in salt-rich phase was carried out through UV-spectroscopy, using a SynergyHT  
123 Microplate Reader, from Biotek, at 803 nm for Cu, 394 nm for Ni and 512 nm for Co,  
124 using calibration curves previously established. The concentration of metals in IL-rich  
125 phase was determined by mass balance. To avoid possible interferences from ABS phase  
126 forming components, blank controls of each ternary system, without metals, were always  
127 prepared and used. The influence of Na<sub>2</sub>SO<sub>4</sub> concentration in metals molar extinction  
128 coefficient was also evaluated and confirmed to be negligible. Three samples of each  
129 phase were analyzed, in at least three individual systems, in order to determine the  
130 partition coefficients ( $K_M$ ) and the respective standard deviations, according to the  
131 following equation,

$$132 \quad K_M = \frac{[M]_{IL}}{[M]_{salt}} \quad (1)$$

134 where  $[M]_{IL}$  and  $[M]_{salt}$  are the concentrations of each metal in the IL- and salt-rich  
135 phases, respectively.

136

### 137 *Metal extraction from acid mine drainage by IL-based ABS*

138 The extraction of metals from AMD was tested in the ABS composed of 25 wt % of IL +  
139 10 wt % of Na<sub>2</sub>SO<sub>4</sub> + 65 wt % of treated AMD with the IL [N<sub>4444</sub>]Cl, [C<sub>4</sub>C<sub>1</sub>im][N(CN)<sub>2</sub>]  
140 and [C<sub>4</sub>C<sub>1</sub>im][SCN], and by using the same experimental procedure described above.  
141 Systems composed of [N<sub>4444</sub>]Cl were prepared by adding NaSCN salt, as adjuvant in the  
142 following molar ratios with total molar amount of Zn present in the treated mine water  
143 (8.2 × 10<sup>-3</sup> mol · L<sup>-1</sup>): 1:0, 1:1, 1:2, 1:5, 1:10, 1:25, 1:50 and 1:68 (Zn:SCN). In these  
144 systems the following mixture point was used: 25 wt % IL + 10 wt % Na<sub>2</sub>SO<sub>4</sub> + 58 wt %  
145 treated AMD + 7 wt % aqueous solution containing variable content of NaSCN. Metal

146 quantification in IL- and salt-rich liquid phases and solid phase was carried-out by total  
147 X-ray fluorescence (TXRF) using a benchtop Picofox S2 (Bruker Nano) spectrometer  
148 with a molybdenum X-ray source. Quartz glass sample carriers were used in TXRF  
149 analysis and pre-treated with 10  $\mu$ L of a solution of silicon in isopropanol and dried in a  
150 heat plate at 80  $^{\circ}$ C for 10 min. IL-rich, salt-rich and solid phase samples were prepared  
151 by mixing 20  $\mu$ L of each phase (solid phase was previously dissolved in 1 mL of pure  
152 ethanol) with 5  $\mu$ L of Y standard solution and 495, 970 and 70  $\mu$ L, respectively, of 1 wt  
153 % polyvinyl alcohol solution. 6.0  $\mu$ L of each mixture was added to treated sample carriers  
154 which were dried in a heat plate at 80  $^{\circ}$ C for 20 min and analyzed in the TXRF  
155 spectrometer for 300 s. A solid phase sample was also analyzed by Fourier transform  
156 infrared (FTIR).

157 The partition coefficients of Al, Cu, Co, Ni and Zn were calculated by using **Eq. (1)**.  
158 Metal precipitation percentage ( $P\%$ ) in solid phase was calculate through the following  
159 equation:

$$160 \quad P\% = \frac{[M]_S \times w_{OH}}{[M]_{AMD} \times w_{AMD}} \times 100$$

161 **(2)**

162 where  $[M]_S$  and  $[M]_{AMD}$  represent, respectively, metal concentration in solid phase and  
163 treated AMD, while  $w_{OH}$  and  $w_{AMD}$  are the weight of pure ethanol used to dissolve solid  
164 phase (0.769 g) and treated AMD added in ABS preparation.

165 The concentration of  $[N_{4444}]Cl$  in the salt-rich phase of each system was determined by  
166  $^1H$  nuclear magnetic resonance (NMR) analysis using a Bruker Advance 300 NMR at 300  
167 MHz, with deuterated dimethyl sulfoxide as the solvent and tetramethylsilane as the  
168 internal reference.

169 IL-rich phase recycling was also studied, and more details are given in the **SI**. Zn and Cu  
170 purity percentages were determined by considering the total amount of metals present in  
171 solid phases, while recovery percentages were calculated taking into account the total  
172 amount of metals present in each system or treated AMD (designated as total recovery).

173

## 174 **Results and Discussion**

### 175 ***AMD composition***

176 AMD sample collected from São Domingos was chemically characterized and the results  
177 obtained are presented in **Table 2**. It presents an acidic pH (1.7) and a high concentration  
178 on sulfates and metals such as Fe, Al, Zn and Cu. Co, Ni, As and Pb were also identified

179 at low concentrations (< 6 ppm) which is in agreement with previous data reported in the  
180 literature concerning São Domingos mine waste.<sup>21,23,24</sup>

181

182 **Table 2.** Characterization of São Domingos AMD original sample and after pretreatment.

	AMD	AMD after pretreatment
<b>pH</b>	1.7	4.0
<b>Conductivity (<math>\mu\text{S}\cdot\text{cm}^{-1}</math>)</b>	7.9	---
<b>Sulfates (<math>\text{g}\cdot\text{L}^{-1}</math>)</b>	11.1	---
<b>Metals (<math>\text{mg}\cdot\text{L}^{-1}</math>)</b>		
<i>Al</i>	546.7	778.0
<i>Fe</i>	715	2.4
<i>Co</i>	3.2	8.0
<i>Ni</i>	1.0	2.7
<i>Cu</i>	82.5	217.8
<i>Zn</i>	210.1	538.4
<i>As</i>	5.8	0.04
<i>Pb</i>	0.1	0.1

183

184 Before metal extraction, the AMD was pre-treated. Water evaporation was carried out  
185 aiming to reduce the total volume of AMD sample and increase the concentration of Al,  
186 Zn, Co, Ni and Cu. This type of procedure is already implemented at industrial level for  
187 lithium extraction from brines to increase the metal concentration before the recovery  
188 step.<sup>25</sup> Here, a total reduction of 67 % of the initial volume was carried leading to an  
189 increase on metals concentration of 3 times, which guarantees that the minimum  
190 concentration required for an adequate detection of metals after extraction (namely those  
191 at very low concentrations).

192 Iron is the most concentrated metal in the AMD sample collected in the mine of São  
193 Domingos. This metal presents high complexation constants when compared with the  
194 remaining transition metals and Al present in AMD, blocking their preferential extraction  
195 by a coordinating agent.<sup>26</sup> Therefore, iron removal from AMD sample before strategic  
196 metals extraction becomes imperative for the development of an efficient process. It is  
197 well known that iron starts to precipitate at lower pH values than other transition metals  
198 in aqueous sulfate-rich solutions. Thus, the selective precipitation of iron by pH  
199 adjustment was evaluated in an AMD concentrated sample with the results shown in  
200 **Figure S2** and **Table S2**. As can be seen in **Figure S2**, metals precipitation efficiency is  
201 highly sensitive to the solution pH. Iron and arsenic present a similar profile and are the

202 metals that reach the highest precipitation efficiency at lower pH value, attaining an  
203 almost complete precipitation (99.91 and 99.82 %, respectively) at pH 4.0. At this pH,  
204 more than 60 % of Al is precipitated, followed by the remaining metals (< 25 % of  
205 precipitation). At a pH around 2.7, it is possible to avoid significant losses of Al, Cu, Co,  
206 Ni and Zn; yet, at these conditions and even with a precipitation efficiency of 78 %, the  
207 iron concentration in AMD would still be high, when compared with the metals of interest  
208 – for example, 2 and 60 times higher than Cu and Co, respectively (*cf.* **Table S2**). Thus,  
209 a compromise was needed and pH 4.0 was selected as the optimum pH to treat the AMD  
210 before the metal extraction step.

211 Metal precipitation from AMD concentrated sample (or any other wastewater sample) is  
212 not only ruled by the solubility of metal hydroxides in water. Since AMD is a sample of  
213 high complexity, with a high amount of solubilized organic matter, this may influence the  
214 metals precipitation. In fact, along with the increase of the pH it was possible to observe  
215 the flocculation of dissolved organic and inorganic matter in the AMD (*cf.* **Figure S2A**).  
216 The complete or partial removal of this organic matter from AMD sample is also  
217 important to guarantee the development of an efficient process. Only close to pH 4.0 it  
218 was possible to obtain a clear water sample (*cf.* **Figure S2B**). The solid formed during  
219 this procedure was collected, treated and analyzed by XRD – **Figure S3**.

220

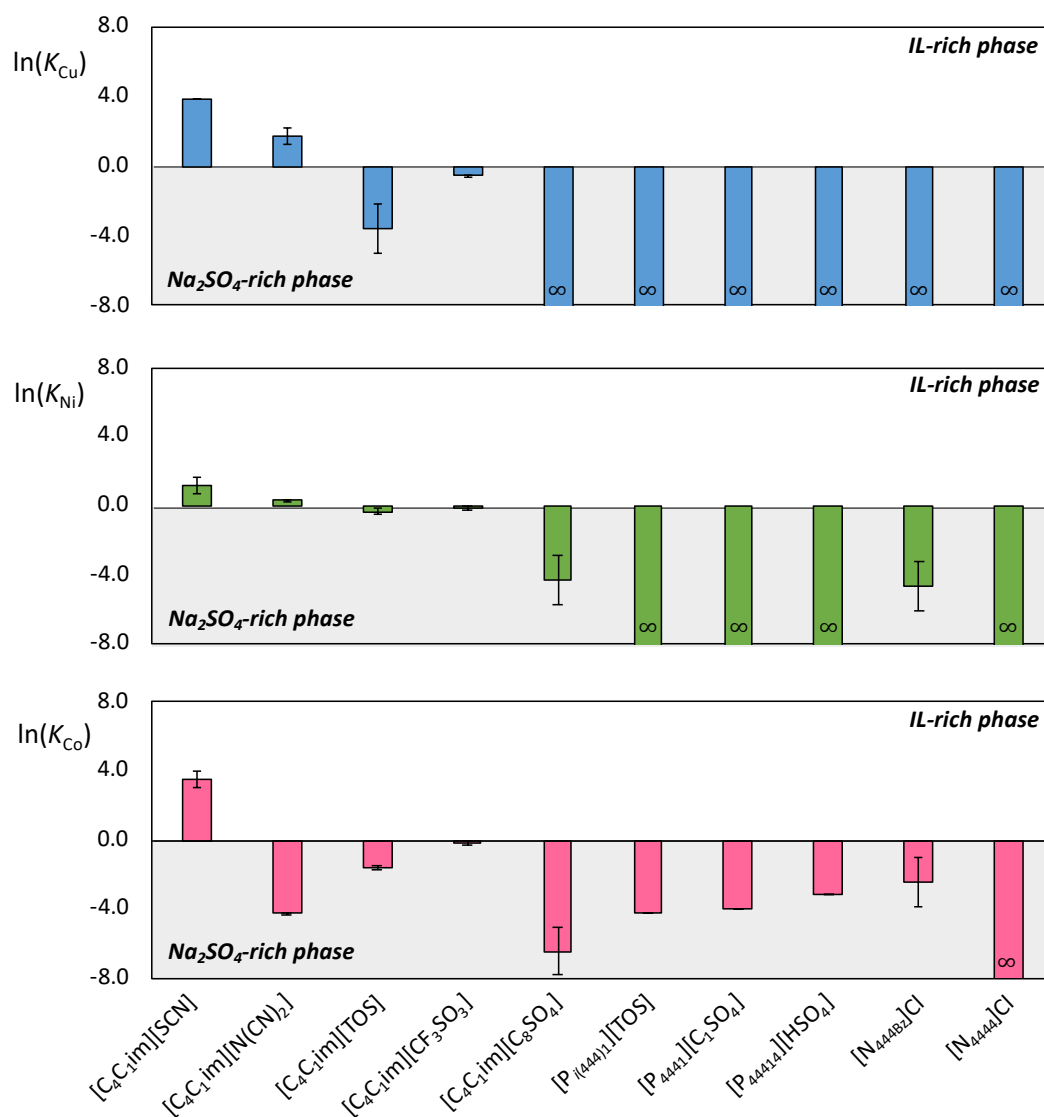
### 221 ***Selection of IL + Na<sub>2</sub>SO<sub>4</sub> + H<sub>2</sub>O ABS for metal extraction***

222 The ability of IL-based ABS to extract Cu, Ni and Co and the influence of IL anion and  
223 cation nature in metal partition, were evaluated. Single metal solutions were used in the  
224 screening, allowing to infer the IL impact on metals partition in the absence of metal  
225 competitive effects. Furthermore, Cu, Ni and Co were selected as representative metals  
226 of AMD composition since their quantification can be easily carried-out by UV-Vis  
227 spectroscopy.

228 Ternary mixtures at the composition of 25 wt % of IL + 10 wt % of Na<sub>2</sub>SO<sub>4</sub> + 65 wt %  
229 of metal aqueous solution were used. This ternary mixture composition was defined by  
230 taking into account the previously reported binodal curves for IL + Na<sub>2</sub>SO<sub>4</sub> ABS,<sup>22</sup> and  
231 choosing a mixture point common to all the biphasic regions. Sodium sulphate was  
232 selected as the salting-out agent since AMD naturally presents a high concentration on  
233 sulfates in its composition (*cf.* **Table 2**). Concerning the 16 IL tested, only the following  
234 were able to induce the formation of ABS when mixed with Na<sub>2</sub>SO<sub>4</sub> in the selected  
235 mixture point: [C<sub>4</sub>C<sub>1</sub>im][SCN], [C<sub>4</sub>C<sub>1</sub>im][N(CN)<sub>2</sub>], [C<sub>4</sub>C<sub>1</sub>im][TOS], [C<sub>4</sub>C<sub>1</sub>im][CF<sub>3</sub>SO<sub>3</sub>],

236 [C<sub>4</sub>C<sub>1</sub>im][C<sub>8</sub>SO<sub>4</sub>], [P<sub>i(444)1</sub>][TOS], [P<sub>4441</sub>][C<sub>1</sub>SO<sub>4</sub>], [P<sub>44414</sub>][HSO<sub>4</sub>], [N<sub>444Bz</sub>]Cl and  
 237 [N<sub>4444</sub>]Cl (*cf.* **Table S1**). Nevertheless, these allowed to evaluate the impact of the IL  
 238 cation (imidazolium, quaternary ammonium and phosphonium) and anion (namely,  
 239 [SCN]<sup>-</sup>, [N(CN)<sub>2</sub>]<sup>-</sup>, [TOS]<sup>-</sup>, Cl<sup>-</sup>) on metal partition.

240 The obtained results for Co, Ni and Cu partition in IL-based ABS are presented in **Figure**  
 241 **1**. Data presented show that only the system composed of the IL [C<sub>4</sub>C<sub>1</sub>im][SCN] was able  
 242 to partition all the three metals preferentially to the IL-rich phase ( $\ln(K_M) > 0$ ). The ABS  
 243 composed of [C<sub>4</sub>C<sub>1</sub>im][N(CN)<sub>2</sub>] was able to extract only Cu and Ni, while  
 244 [C<sub>4</sub>C<sub>1</sub>im][CF<sub>3</sub>SO<sub>3</sub>]-based ABS presented an equal distribution of metals between the  
 245 system phases ( $\ln(K_M) \sim 0$ ). All the remaining biphasic systems showed no metal  
 246 extraction for IL-rich phase ( $\ln(K_M) < 0$ ). Importantly, no metal precipitation in any of  
 247 the systems studied was observed.



248

249 **Figure 1.** IL effect in the partition coefficient ( $K_M$ ) of Cu, Co and Ni in ABS composed  
250 of 25 wt % of IL + 10 wt % of  $\text{Na}_2\text{SO}_4$  + 65 wt % of metal aqueous solution at  $(25 \pm 1)$   
251 °C and atmospheric pressure.

252

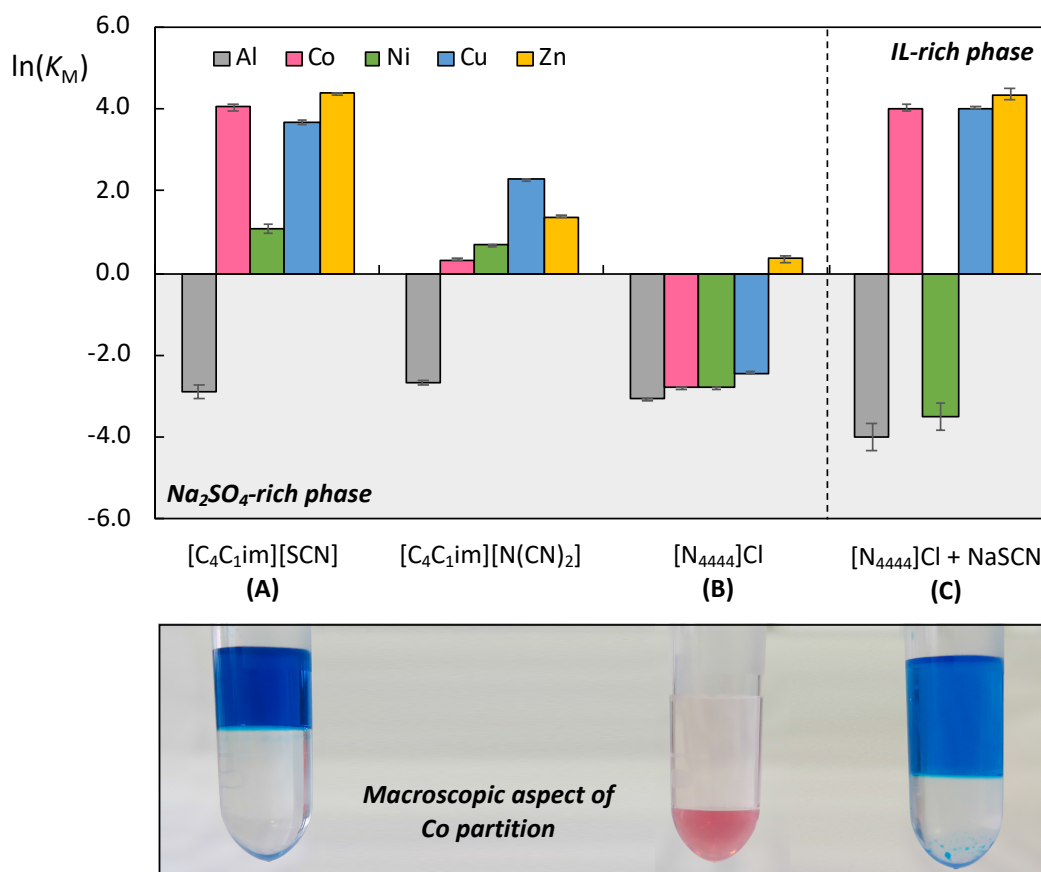
253 Metal extraction in ABS systems may occur through the formation of negatively charged  
254 metal complexes with inorganic anions in the absence of an extractant.<sup>27</sup> Among them,  
255 halides and  $[\text{SCN}]^-$  are commonly used as extracting agents. Thiocyanate is an  
256 ambidentate ligand, *i.e.*, it coordinates with metals through either the nitrogen and/or  
257 sulfur atom, and its ability to coordinate with metals such as Co, Ni and Cu is well  
258 established in literature and explains the results obtained for metals extraction by using  
259  $[\text{C}_4\text{C}_{1\text{im}}][\text{SCN}]$ -based ABS (*cf.* **Figure 1**).<sup>28–31</sup> Considering the first complexation  
260 constants of these metals with  $\text{SCN}^-$  the following trend was expected to be observed:  
261  $\text{Cu}^{2+}$  ( $\log\beta_1 = 1.7$ ) >  $\text{Ni}^{2+}$  ( $\log\beta_1 = 1.14$ ) >  $\text{Co}^{2+}$  ( $\log\beta_1 = 1.01$ ).<sup>26</sup> However, while Cu and  
262 Co are extracted in the form of tetrahedral metal-thiocyanate complexes –  $\text{Cu}(\text{SCN})_4^{2-}$   
263 and  $\text{Co}(\text{SCN})_4^{2-}$  – which are rarely formed in aqueous solution, Ni is known to stay in the  
264 form of octahedral complex anion, which present a more hydrophilic character and, thus,  
265 a lower partition to the IL-rich phase. These results are also supported by the comparison  
266 of UV-Vis spectra of metals in IL-rich phase and aqueous solution presented in **Figure**  
267 **S4**.  $[\text{N}(\text{CN})_2]$ -based ILs ability to extract metals in two liquid phases systems was also  
268 previously demonstrated.<sup>32,33</sup> Similar to  $[\text{SCN}]^-$  anion,  $[\text{N}(\text{CN})_2]^-$  also presents a high  
269 ability to interact with metallic cations through the formation of stable metal complexes.  
270 Furthermore, the trend observed on metal partitions in  $[\text{C}_4\text{C}_{1\text{im}}][\text{N}(\text{CN})_2]$ -based ABS –  
271  $K_{\text{Cu}} > K_{\text{Ni}} \gg K_{\text{Co}}$  – is in good agreement with data previously reported.<sup>33</sup> Thus, it seems  
272 clear that IL-based ABS ability to extract metals such as Ni, Co and Cu, to IL-rich phase  
273 is mainly ruled by the IL anion nature, while the partition extension is related to the type  
274 and stability of metal complexes that are formed between metal cation and IL anion.  
275 Among all the systems evaluated only those composed of  $[\text{SCN}]^-$  and  $[\text{N}(\text{CN})_2]^-$  were  
276 able to extract metals to the IL-rich phase, being thus selected as the best candidates to  
277 the metals extraction from AMD.

278

### 279 ***Metal extraction from AMD real sample by IL-based ABS***

280 ABS composed of  $\text{Na}_2\text{SO}_4$  and the ILs  $[\text{C}_4\text{C}_{1\text{im}}][\text{SCN}]$ ,  $[\text{C}_4\text{C}_{1\text{im}}][\text{N}(\text{CN})_2]$  and  $[\text{N}_{4444}]\text{Cl}$   
281 were tested in metal extraction from treated AMD sample.  $[\text{N}_{4444}]\text{Cl}$ -based ABS showed  
282 no metal extraction when single metal aqueous solutions were used (*cf.* **Figure 1**).

283 Nevertheless, to guarantee that AMD composition is not affecting the trends previously  
 284 observed, this IL was also considered in these experiments. It is also important to note  
 285 that, when dealing with metal extraction from AMD, the sulfate present in the system  
 286 needs to be taken into account; nevertheless, it represents only 7.3 % of the total amount  
 287 of  $\text{Na}_2\text{SO}_4$  (0.72 wt % of mixture point composition) needed to induce the phases  
 288 separation, being always necessary to add 9.3 wt % more sulfate salt to the mixture. The  
 289 results obtained are presented in **Figure 2**.



290  
 291

292 **Figure 2.** Metal extraction from AMD treated sample by using IL +  $\text{Na}_2\text{SO}_4$  +  $\text{H}_2\text{O}$  ABS  
 293 at pH 4 and  $(298 \pm 1)$  K: metal partition coefficients,  $\ln(K_M)$  (at the top) and macroscopic  
 294 aspect of Co partition in the identified systems (at the bottom).

295

296 The extractions of Al, Co, Ni, Cu and Zn from pretreated AMD sample in IL-based ABS  
 297 were experimentally assessed. The following trends were observed for the partition  
 298 coefficients:  $\text{Zn} > \text{Co} > \text{Cu} \gg \text{Ni} > \text{Al}$  in  $[\text{C}_4\text{C}_1\text{im}][\text{SCN}]$ -,  $\text{Cu} > \text{Zn} > \text{Ni} > \text{Co} > \text{Al}$  in  
 299  $[\text{C}_4\text{C}_1\text{im}][\text{N}(\text{CN})_2]$ -, and no metal extraction was observed in the  $[\text{N}_{4444}]\text{Cl}$ -based system.  
 300 For Cu, Co and Ni, the results obtained are in good agreement with those obtained when

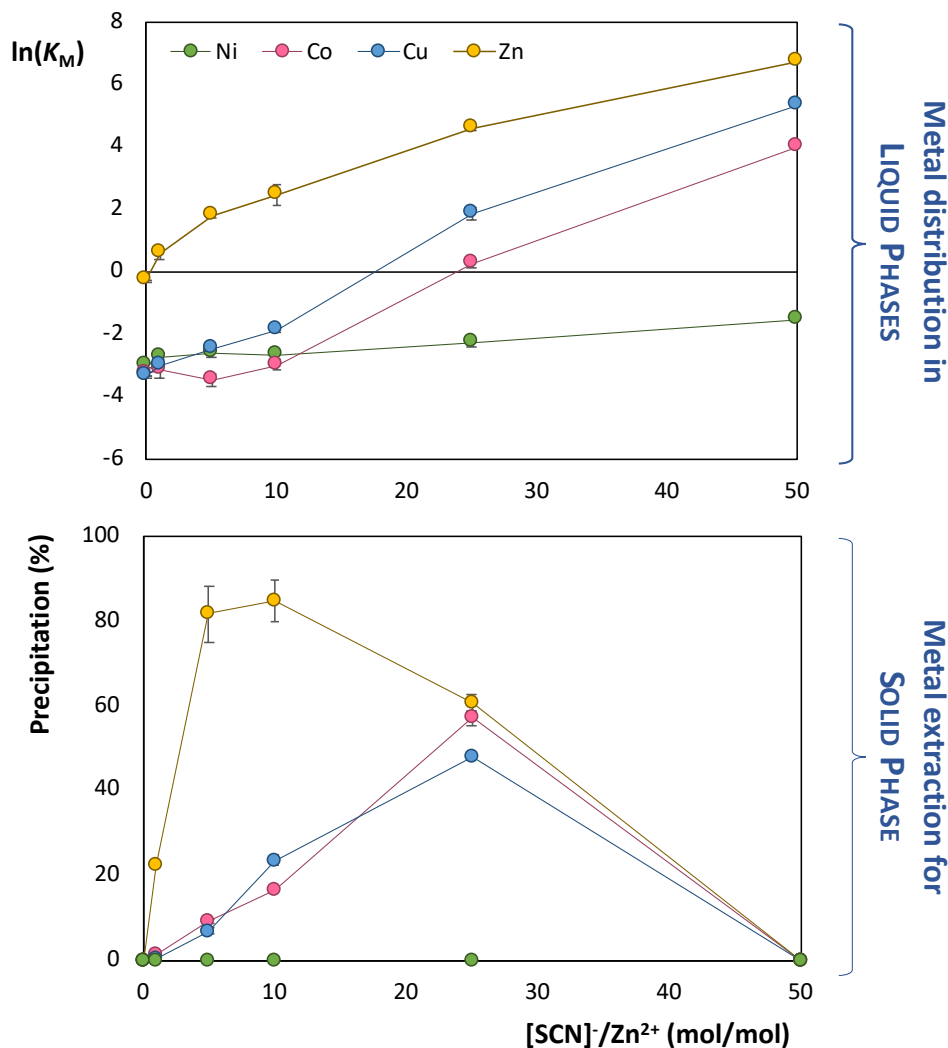
301 single-metal aqueous solutions were considered at the same conditions (*cf.* **Figure 1**). In  
302 what concerns Zn and Al, IL-based ABS composed of [C<sub>4</sub>C<sub>1</sub>im][SCN] and  
303 [C<sub>4</sub>C<sub>1</sub>im][N(CN)<sub>2</sub>] were able to induce the preferential partition of Zn to the IL-rich  
304 phase, while there were no systems capable to extract Al. Al is not able to form anionic  
305 complexes in presence of any of these ions. In fact, only the hydrophilic complex  
306 [Al(SCN)(H<sub>2</sub>O)<sub>5</sub>]<sup>2+</sup> was reported for temperature and ionic strength conditions similar to  
307 the tested system – which may justify its preferential partition to the salt-rich phase.<sup>34</sup>

308

### 309 *Selective extraction of strategic metals from AMD*

310 The relatively high costs associated to imidazolium-based ILs may create limitations to  
311 their use at industrial scale. Quaternary ammonium-based ILs are much less expensive  
312 than their imidazolium-based counterparts and, generally, present also a lower  
313 environmental impact.<sup>35</sup> In **Figure 2** are also presented the results obtained for metal  
314 extraction from treated AMD by using an ABS composed of Na<sub>2</sub>SO<sub>4</sub>, [N<sub>4444</sub>]Cl and 2.0  
315 wt % of NaSCN. The observed results are quite interesting since metal partition  
316 coefficients similar to those obtained with the [C<sub>4</sub>C<sub>1</sub>im][SCN]-based system were  
317 obtained in a system that was previously shown to be unable to extract metals. It is  
318 expected that a similar result can be obtained if the IL [N<sub>4444</sub>][SCN] is directly used.  
319 However, the addition of thiocyanate anion to the system in the form of NaSCN presents  
320 some advantages: (i) it allows to reduce the costs of the system since it is less expensive  
321 to use NaSCN (~0.32 €/g at Sigma-Aldrich) and [N<sub>4444</sub>]Cl (~2.5 €/g at Sigma Aldrich)  
322 than [N<sub>4444</sub>][SCN] (~4.8 €/g at Sigma-Aldrich), (ii) it allows to reduce system  
323 environmental impact, being possible to control the amount of [SCN]<sup>-</sup> added and reduce  
324 it up to the minimum necessary to achieve the desired metal extraction, and (iii) it allows  
325 tunable metal selectivity controlled by the concentration of [SCN]<sup>-</sup> added to the ABS, as  
326 will be demonstrated further.

327 As previously referred, metal extraction by coordinating ions such as [SCN]<sup>-</sup> is ruled by  
328 the formation of stable complexes, better extracting those metals that present high  
329 complexation constants and result in complexes of more stable conformation. Thus, metal  
330 selectivity may be controlled by the amount of coordination anion added to the system.  
331 The effect of thiocyanate anion concentration on metals partition from AMD sample was  
332 evaluated and the results obtained are presented in **Figure 3**. The maximum amount of  
333 Zn (the most concentrated metal in treated AMD sample) was considered as reference to  
334 define the amount of [SCN]<sup>-</sup> to be added to the ABS.



335

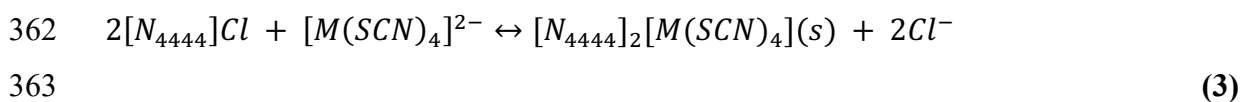
336 **Figure 3.** Thiocyanate molar ratio effect on metal extraction from AMD sample: [SCN]<sup>-</sup>  
 337 influence in metal partition between IL- and salt-rich liquid phases,  $\ln(K_M)$ , (at the top)  
 338 and in metals precipitation percentage (at the bottom).

339

340 The trend observed for metal partition coefficients between IL- and salt-rich liquid phases  
 341 is maintained in the whole range of [SCN]<sup>-</sup> concentrations studied. Zn is the most  
 342 extracted metal followed by Cu and Co, while Ni is not extracted to the IL-rich phase  
 343 independently of [SCN]<sup>-</sup> concentration. Due to limitations on Al quantification by TXRF,  
 344 the partition of this metal was not determined here; still, it was previously demonstrated  
 345 that this system is not able to extract Al (*cf.* **Figure 2**). It is also clear that [SCN]<sup>-</sup>  
 346 concentration has a significant impact on metal separation efficiency, being possible to  
 347 tune the system for the selective separation of different metal pairs.

348 Unexpectedly, in the ABS composed of [SCN]<sup>-</sup>/ Zn<sup>2+</sup> molar factors between 1 and 25 the  
 349 formation of a dark red colored precipitate was observed (*cf.* **Figure S5** in the **SI**), with

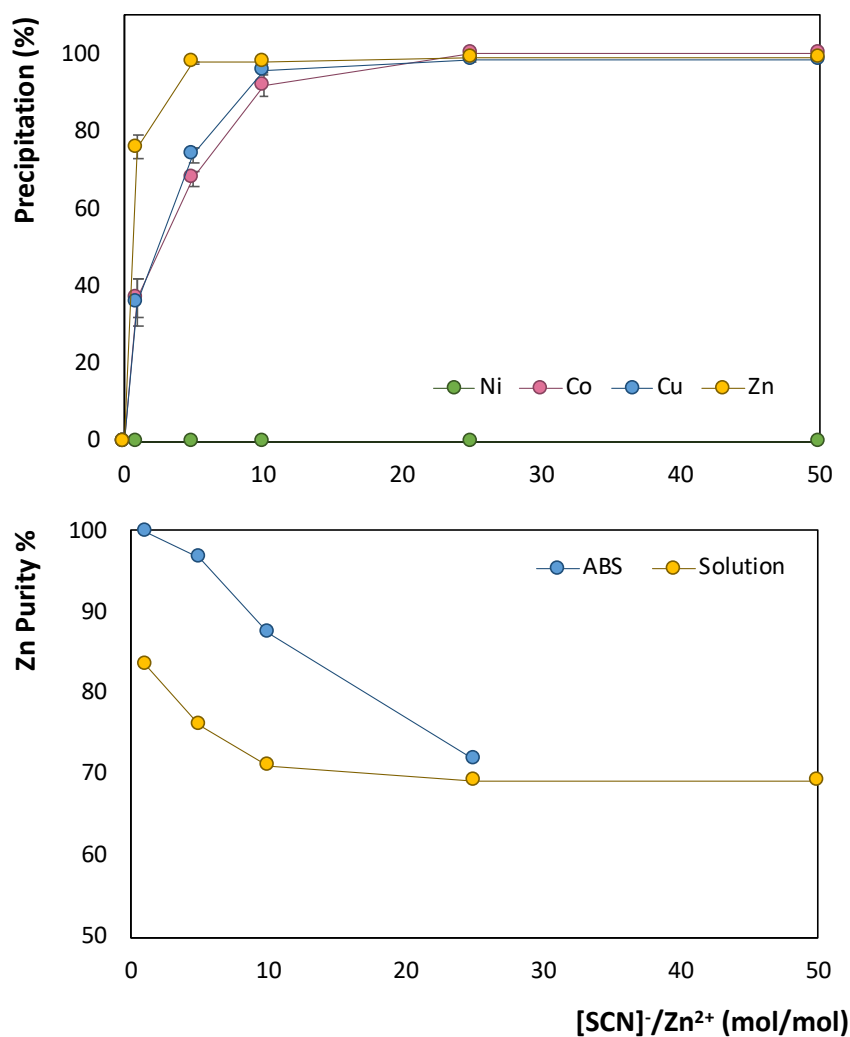
350 the Zn, Cu and Co extracted metals partitioning between the IL-rich phase and precipitate  
 351 as shown in **Figure 3**. The occurrence of this type of solid phases in liquid-liquid systems  
 352 composed of ILs was previously reported and used for metals recovery, namely platinum,  
 353 gold and palladium.<sup>36-38</sup> Under certain conditions depending on the IL and ligand  
 354 concentration, mixed metallic organic precipitate can occur with IL cations compensating  
 355 for the charge of the anionic metal complex. In the studied system, precipitation occurs  
 356 when both  $[N_{4444}]Cl$  and  $NaSCN$  are mixed together with treated AMD sample  
 357 independently of  $Na_2SO_4$  addition. The FTIR spectra of the resulted precipitate is  
 358 presented in **Figure S6** and clearly shows that the IL cation and thiocyanate anion are co-  
 359 precipitating with the transition metals. These results suggest that the formation of  
 360  $[N_{4444}]_2[M(SCN)_4]$  is occurring and precipitation can be thus represented according to  
 361 **Eq. (3)**:<sup>38</sup>



364 Despite 4 mols of  $[SCN]^-$  being necessary to form the IL metalate complex presented in  
 365 **Eq. (3)**, solid phase and red colored IL-rich liquid phase were observed at lower ratios  
 366 (1:1). Thus, the possibility that  $Cl^-$  anions participate also in this reaction cannot be  
 367 excluded and an organic metal complex of the type  $[N_{4444}]_2[M(SCN)_X(Cl)_Y]$  may be  
 368 occurring, with  $X$  and  $Y$  ratio changing with the amount of  $[SCN]^-$  added to the ABS.  
 369 More experimental work is needed to clarify the mechanism and the type of complex that  
 370 is occurring at these conditions. At  $[SCN]^-$  higher concentrations the IL-metalate complex  
 371 solubility in IL-rich phase increases and becomes completely soluble, with no  
 372 precipitation occurring at  $[SCN]^-/Zn^{2+} \geq 50$  (*cf.* **Figures 3** and **S5**).

373 Data presented in **Figure 3** shows that when precipitation occurs it is possible to recover  
 374 more than 80 % of the total Zn present in the AMD with high selectivity. The question  
 375 therefore arises, is there any advantage to using an ABS over direct precipitation? To  
 376 address this, metal precipitation percentage in homogeneous mixtures of AMD for the  
 377 same  $[N_{4444}]Cl$  and  $NaSCN$  ratio in the absence of  $Na_2SO_4$  was determined and compared  
 378 to those using ABS, the obtained results are presented in the **Figure 4**. Remarkably,  
 379 almost 100 % of Co, Cu and Zn precipitation is achieved when AMD is mixed only with  
 380 IL and thiocyanate salt, allowing for higher metal recovery percentages when compared  
 381 with those obtained in the ABS phase (*cf.* **Figure 3**). However, by considering Zn purity  
 382 in the solid phase – **Figure 4** – it is possible to conclude that the precipitation in  
 383 homogenous solutions results in decreased Zn purity in the precipitate. When ABS are

384 induced by the addition of Na<sub>2</sub>SO<sub>4</sub> to the homogenous mixtures, anionic metal complex  
 385 solubility in IL-rich liquid phase increases due to the decrease of water concentration.  
 386 This is visually evident by the increase of IL-rich phase red color (*cf.* **Figure S5**). At the  
 387 same time, the selectivity is improved and the Zn purity percentages of 99.7 % can be  
 388 reached at low [SCN]<sup>-</sup> concentrations. These results suggest that IL-based ABS can be  
 389 used to develop a process for the sequential selective extraction and simultaneous  
 390 recovery of transition metals from AMD.



391  
 392 **Figure 4.** Thiocyanate molar ratio effect on metal precipitation from AMD sample in  
 393 homogenous mixtures composed AMD + IL + aqueous solution of NaSCN (at the top)  
 394 and on Zn purity percentage in the solid phase obtained in homogenous mixtures  
 395 (*Solution*) and ABS at the same conditions (at the bottom).

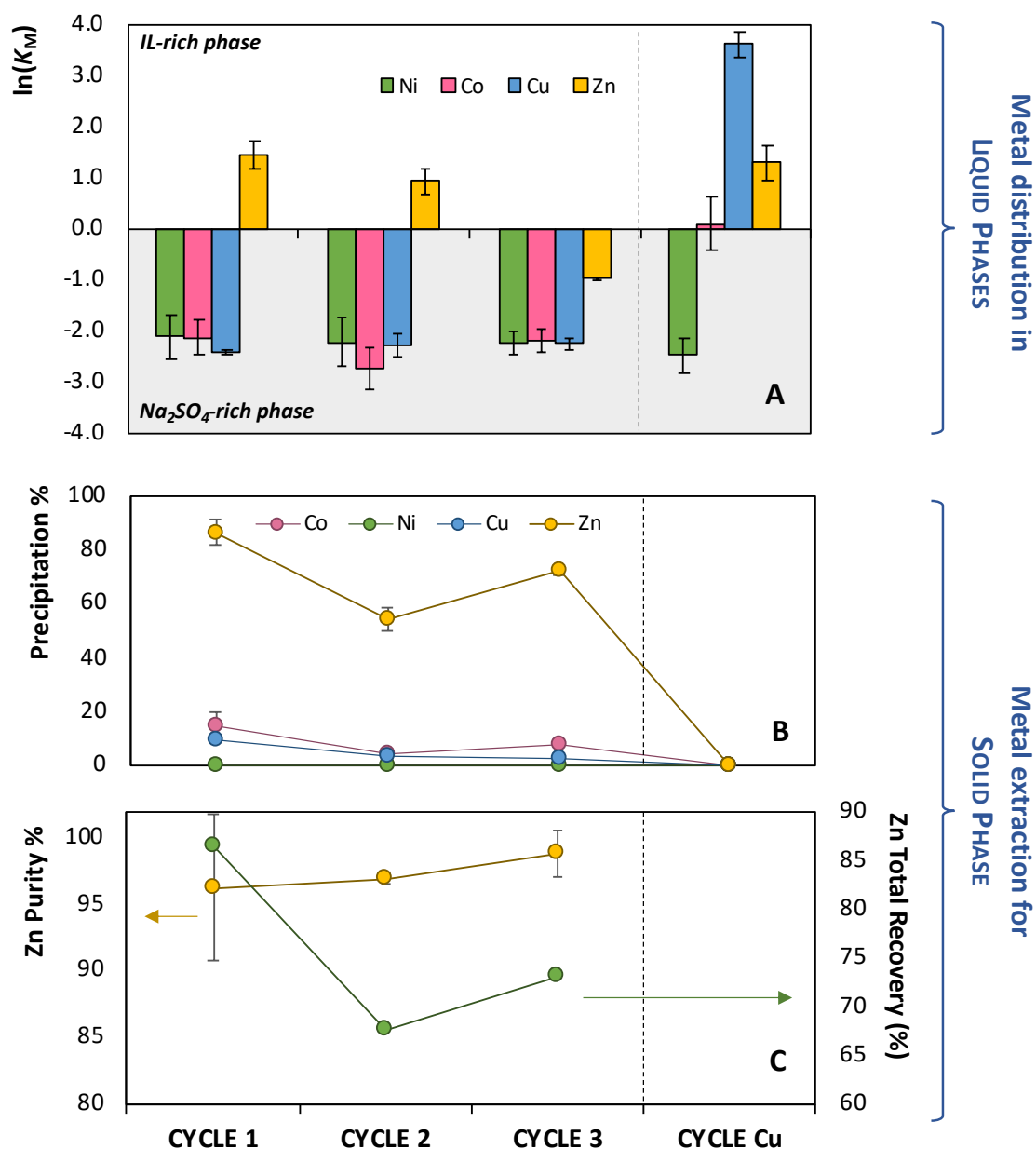
396  
 397 Considering that Zn is the most concentrated metal in AMD and the first to be extracted  
 398 in ABS (higher complexation constant), searching for a balance between the percentage

399 of Zn that is extracted in solid-phase and its final purity,  $[\text{SCN}]^-/\text{Zn}^{2+}$  molar factor of 5  
400 seems to be the best option for Zn recovery, resulting in 81.6 % of Zn precipitation with  
401 95.3 % of purity in a single extraction/recovery step (*cf.* **Figures 3** and **4**). Furthermore,  
402 at this ratio only Zn is partitioned to the IL-rich phase ( $\ln(K_M) > 0$ ), while Ni and most part  
403 of Cu and Co (> 91 % of total metal amount) remain in salt-rich phase, allowing for the  
404 sequential extraction of the remaining metals. Nevertheless, aiming at the development  
405 of a sustainable process it is important to consider and study the reuse and recycling of  
406 the main chemicals/solvents used. Thus, the reuse of IL-rich phase for several extraction  
407 steps without the addition of extra amount of  $[\text{SCN}]^-$  and the reuse of salt-rich phase for  
408 the sequential extraction of Cu was evaluated.

409

#### 410 ***IL- and salt-rich phases reuse in consecutive cycles of extraction***

411 To optimize the selective extraction and simultaneous recovery of Zn over the remaining  
412 metals present in the AMD sample, 3 consecutive cycles were carried out and the results  
413 obtained are presented in **Figure 5**.



414

415 **Figure 5.** Zn extraction and recovery from treated AMD by using the recycled IL-rich  
 416 phase for 3 cycles (CYCLE 1, 2 and 3) and salt-rich phase to Cu extraction (CYCLE Cu):  
 417 (A) metal partition coefficients in ABS liquid phases,  $\ln(K_M)$ ; (B) metal precipitation  
 418 percentage; (C) Zn purity % in the solid phase (yellow) and Zn total recovery % (green).  
 419

420 The first extraction step was carried-out at the conditions previously considered as the  
 421 best for the simultaneous extraction and recovery of Zn ( $[\text{SCN}]^-/\text{Zn}^{2+} = 5$ ). The cycles 2  
 422 and 3 were induced by adding Na<sub>2</sub>SO<sub>4</sub> (10 wt %, to induce phase separation) and fresh  
 423 AMD treated sample (in the amount required to fulfill the system initial weight), to the  
 424 IL-rich phase collected from the previous system. The results obtained for these 3 cycles  
 425 demonstrate that, without the addition of NaSCN, the Zn preferential partition to the IL-

426 rich liquid phase decreases. Nevertheless, Zn precipitation percentage was always  
427 significantly higher than remaining metals and its purity in the solid phase increased along  
428 the cycles, reaching a maximum of 98.8 % in cycle 3 – *cf.* **Figure 5**. Furthermore,  
429 considering the total amount of AMD used in the 3 cycles of extraction/recovery, 73.1 %  
430 of total Zn was recovered in solid phase. This means that with the amount of IL added in  
431 the first extraction/recovery cycle it is possible to extract (at least) 2.1 times more Zn than  
432 if a single extraction step was used, reducing the process cost and environmental impact.  
433 This is also achieved with a very small amount of SCN-based salt, which was added to  
434 the system only in the first extraction step (cycle 1). This suggests that, after the first  
435 extraction there is still free [SCN]<sup>-</sup> anion in IL-rich liquid phase to form complexes with  
436 the novel metal loading introduced in the cycle 2 and 3. However, the decrease of [SCN]<sup>-</sup>  
437 /Zn molar ratio as a significant impact on the preferential partition of Zn to IL-rich liquid  
438 phase (*cf.* **Figure 5A**).

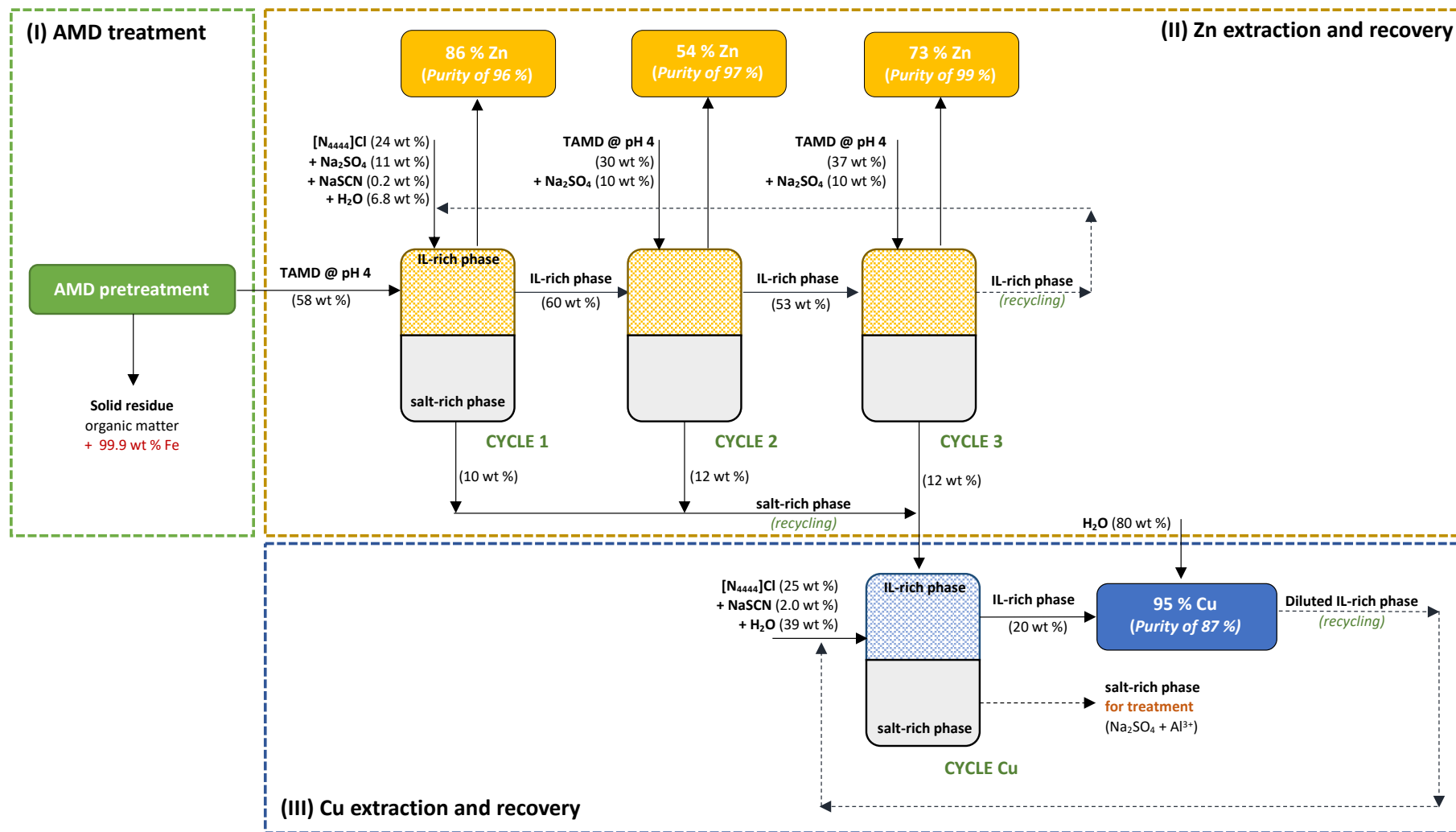
439 It is also important to note that IL losses during IL-rich phase recycling should be low –  
440 after the first cycle 2.1 % of the IL total amount is lost to salt-rich phase – due to the  
441 impact of thiocyanate addition to the system (more details are discussed in **SI**).  
442 Furthermore, considering that there is no co-precipitation of IL beyond the IL metalate  
443 complex in the solid phase, it is possible to estimate that the total amount of IL lost in the  
444 three extraction cycles in the form of insoluble organic metal is < 0.6 % of the initial  
445 amount of IL used to induce the first cycle.

446 After each extraction cycle there is a new salt-rich phase almost free of Zn and rich in the  
447 remaining metals, namely Cu. From the previous results, Cu is the metal, after Zn, with  
448 higher extraction, meaning that in the absence of Zn, Cu will be selectively extracted to  
449 the IL-rich if the correct ratio between Cu and [SCN]<sup>-</sup> anions is selected (*cf.* **Figure 3**).  
450 Thus, a last extraction cycle (designated as CYCLE Cu) was carried-out by collecting and  
451 mixing the three salt-rich phases that resulted from cycle 1 to 3 and by adding the same  
452 amount of IL (~25 wt %) added to induce the first extraction step (CYCLE 1) and excess  
453 NaSCN (2 wt %). Since most part of Cu (together with Co and Ni) loaded in each previous  
454 cycle was concentrated in the salt-rich phases, and almost no Zn was present, the increase  
455 of [SCN]<sup>-</sup> concentration was enough to result in the preferential and selective partition of  
456 Cu to the IL-rich phase, as presented in **Figure 5**. However, as previously observed, at  
457 this concentration of [SCN]<sup>-</sup> there is no formation of solid phase and Cu recovery requires  
458 an additional recovery step.

459

460 **Discussion**

461 The obtained results lead us to the conceptual development of a novel process which  
462 allows the sequential selective separation of strategic metals from AMD, as presented in  
463 **Figure 6**. This process is divided in three main steps: (i) the AMD treatment for metals  
464 concentration and Fe and organic matter precipitation by evaporation and pH adjustment,  
465 (ii) the selective extraction and simultaneous recovery of Zn from AMD by IL-based ABS  
466 and (iii) the selective extraction and recovery of Cu from the salt-rich phase. All data  
467 presented in **Figure 6** was obtained from the study on IL- and salt-rich phases reuse  
468 discussed above (*cf.* **Figure 5**). Process steps concerning IL-rich phase recycling to initial  
469 extraction steps were not experimentally tested. Still, the results obtained in this work and  
470 previously reported data can support the feasibility of proposed process as it will be  
471 discussed further.



472

473 **Figure 6.** Process diagram of the sequential selective extraction and recovery of strategic metals from AMD real sample by using IL-based ABS. The IL  
 474 recycling in new extraction cycles are theoretically described (process diagram described with dashed lines was not performed experimentally). *TAMD*:  
 475 treated AMD.

476 The proposed process starts with AMD treatment by evaporation and pH adjustment. The  
477 evaporation in São Domingos, considering the favorable environmental conditions  
478 presented by the location, could be carried in open-air pounds. Treated AMD at pH 4.0 is  
479 obtained, as well as a waste stream that consists in Fe-rich sludge. Then, treated AMD  
480 proceeds to metal selective extraction step. Here three cycles of selective precipitation of  
481 Zn are sequentially applied, by reusing the IL-rich phase and introducing fresh treated  
482 AMD and  $\text{Na}_2\text{SO}_4$  in each cycle (*cf.* **Figure 5**). Salt-rich phases obtained after each Zn  
483 extraction and recovery cycle are collected to a new extraction system, in which fresh IL  
484 and NaSCN are added to induce phase separation, allowing the selective extraction of Cu  
485 as previously demonstrated (*cf.* **Figure 5**). After extraction step, 95 % of Cu present in  
486 IL-rich phase (representing 46.3 % of the total Cu introduced in the full process) is  
487 recovered in the form of organic-metal complex by IL-rich phase dilution in water (at 1:5  
488 mass ratio), with a purity of 87 %. Metals recovery allows to regenerate the IL-rich  
489 phases, allowing their reuse with minimal additional treatment to induce novel ABS and,  
490 consequently, reduce the amount of fresh IL added in the first cycle of Zn and Cu  
491 extraction ultimately leading to a more sustainable process.

492 Co and Ni concentrations are too low in the collected AMD (*cf.* **Table 1**) for their  
493 extraction be economically viable, despite their market price. Still, this process showed a  
494 high versatility and dynamism, induced by tunable character of IL-based ABS, and  
495 meaning that, in the presence of other AMD or similar wastewater richer in these valuable  
496 metals, the process can be optimized aiming their recovery.

497

## 498 **Conclusion**

499 The separation of Zn, Al, Cu, Co and Ni from real AMD water sample collected in São  
500 Domingos Portuguese mine was here studied. The selective sequential recovery of these  
501 strategic metals from AMD by using IL-based ABS was successfully demonstrated. It  
502 was shown that their ability to extract metals is mainly ruled by IL anion, while the  
503 partition coefficient is related with the formation of metal complexes of stable  
504 conformation. The [SCN]-based IL presented the best results for metal extraction.  
505 However, the system composed of  $[\text{N}_{4444}]\text{Cl} + \text{Na}_2\text{SO}_4 + \text{H}_2\text{O}$  with the addition of small  
506 and controlled amounts of NaSCN was shown to be the most promising, since it allowed  
507 to tune metal selective extraction and simultaneous recovery by adjusting the amount of  
508  $[\text{SCN}]^-$  added, and the development of a more cost-effective and sustainable process. The  
509 results obtained led to the conceptual development of a novel process for the selective

510 sequential extraction and recovery of Zn and Cu from AMD. In this process, 73.1 % of  
511 Zn present in treated AMD can be recovered with 98.8 % of purity, after three extraction  
512 cycles with IL-rich phase recycling and with no addition of extra amount of  $[\text{SCN}]^-$  and  
513 no need of an extra recovery step. Cu is extracted in a last step from the salt-rich phases  
514 collected from Zn extraction systems and its recovery is carried-out by precipitation of  
515 water insoluble IL metalate complex. The high tunable character of IL-based ABS confers  
516 to this process a high versatility, being possible to optimize it for the recovery of other  
517 strategic metals from different wastewaters. The proposed process appears as a promising  
518 strategy to the recovery of strategic metals from metal containing wastes, allowing to add  
519 value to treatment processes whilst simultaneously addressing an environmental problem  
520 if left untreated.

521

## 522 **Acknowledgements**

523 This work was developed within the scope of the project CICECO-Aveiro Institute of  
524 Materials, UIDB/50011/2020 & UIDP/50011/2020, financed by national funds through  
525 the Foundation for Science and Technology/MCTES. Field work and geochemical  
526 analysis were financed by the GeoBioTec Research Unit. This work is funded by national  
527 funds through FCT – Fundação para a Ciência e a Tecnologia, I.P., under the Scientific  
528 Employment Stimulus - Individual Call - CEECIND/00831/2017 - under the CEEC  
529 Individual 2017.

530

## 531 **Supporting Information**

532 The Supporting Information is available free of charge and includes the detailed list of  
533 chemicals and instruments used, experimental details and analysis of AMD treatment and  
534 IL-rich phase recycling, XRD diffractograms of the obtained precipitate after AMD pH  
535 adjustment, UV-Vis spectra of metal at different experimental conditions, macroscopic  
536 aspect of ABS at different thiocyanate concentrations, FTIR and UV-Vis spectra of IL  
537 metalate complex, binodal curve of the ternary system  $[\text{N}_{4444}]\text{Cl} + \text{Na}_2\text{SO}_4 + \text{H}_2\text{O}$  with  
538 and without the addition of NaSCN, effect of thiocyanate anion on IL concentration in  
539 the salt-rich phase.

540

## 541 **References**

542 (1) European Commission, *Critical Raw Materials Resilience: Charting a Path*  
543 *towards Greater Security and Sustainability (COM/2020/474 Final)*; Brussels,

- 544 2020.
- 545 (2) Graedel, T. E.; Harper, E. M.; Nassar, N. T.; Nuss, P.; Reck, B. K. Criticality of  
546 Metals and Metalloids. *Proc. Natl. Acad. Sci. U. S. A.* **2015**, *112*, 4257–4262. DOI:  
547 10.1073/pnas.1500415112.
- 548 (3) Park, I.; Tabejin, C. B.; Jeon, S.; Li, X.; Seno, K.; Ito, M.; Hiroyoshi, N. A Review  
549 of Recent Strategies for Acid Mine Drainage Prevention and Mine Tailings  
550 Recycling. *Chemosphere* **2019**, *219*, 588–606. DOI:  
551 10.1016/j.chemosphere.2018.11.053.
- 552 (4) Naidu, G.; Ryu, S.; Thiruvengkatachari, R.; Choi, Y.; Jeong, S.; Vigneswaran, S. A  
553 Critical Review on Remediation, Reuse, and Resource Recovery from Acid Mine  
554 Drainage. *Environ. Pollut.* **2019**, *247*, 1110–1124. DOI:  
555 10.1016/j.envpol.2019.01.085.
- 556 (5) Wei, X.; Zhang, S.; Shimko, J.; Dengler, R. W. Mine Drainage: Treatment  
557 Technologies and Rare Earth Elements. *Water Environ. Res.* **2019**, *91*, 1061–1068.  
558 DOI: 10.1002/wer.1178.
- 559 (6) Rambabu, K.; Banat, F.; Pham, Q. M.; Ho, S.-H.; Ren, N.-Q.; Show, P. L.  
560 Biological Remediation of Acid Mine Drainage: Review of Past Trends and  
561 Current Outlook. *Environ. Sci. Ecotechnology* **2020**, *2*, 100024. DOI:  
562 10.1016/j.ese.2020.100024.
- 563 (7) Kefeni, K. K.; Msagati, T. A. M.; Mamba, B. B. Acid Mine Drainage: Prevention,  
564 Treatment Options, and Resource Recovery: A Review. *J. Clean. Prod.* **2017**, *151*,  
565 475–493. DOI: 10.1016/j.jclepro.2017.03.082.
- 566 (8) MacIngova, E.; Luptakova, A. Recovery of Metals from Acid Mine Drainage.  
567 *Chem. Eng. Trans.* **2012**, *28*, 109–114. DOI: 10.3303/CET1228019.
- 568 (9) Yan, B.; Mai, G.; Chen, T.; Lei, C.; Xiao, X. Pilot Test of Pollution Control and  
569 Metal Resource Recovery for Acid Mine Drainage. *Water Sci. Technol.* **2015**, *72*,  
570 2308–2317. DOI: 10.2166/wst.2015.429.
- 571 (10) Chen, T.; Yan, B.; Lei, C.; Xiao, X. Pollution Control and Metal Resource  
572 Recovery for Acid Mine Drainage. *Hydrometallurgy* **2014**, *147–148*, 112–119.  
573 DOI: 10.1016/j.hydromet.2014.04.024.
- 574 (11) Kefeni, K. K.; Msagati, T. M.; Mamba, B. B. Synthesis and Characterization of  
575 Magnetic Nanoparticles and Study Their Removal Capacity of Metals from Acid  
576 Mine Drainage. *Chem. Eng. J.* **2015**, *276*, 222–231. DOI:  
577 10.1016/j.cej.2015.04.066.

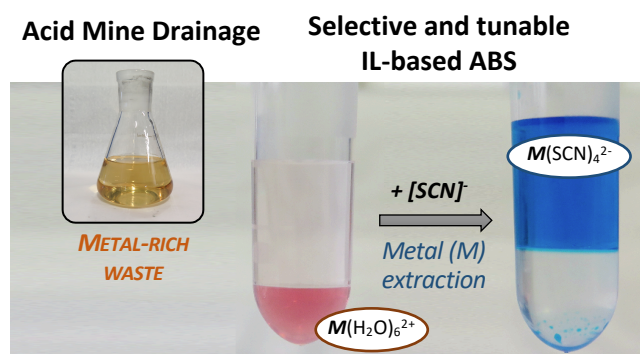
- 578 (12) Larsson, M.; Nosrati, A.; Kaur, S.; Wagner, J.; Baus, U.; Nydén, M. Copper  
579 Removal from Acid Mine Drainage-Polluted Water Using Glutaraldehyde-  
580 Polyethyleneimine Modified Diatomaceous Earth Particles. *Heliyon* **2018**, *4*,  
581 e00520. DOI: 10.1016/j.heliyon.2018.e00520.
- 582 (13) Ayora, C.; Macías, F.; Torres, E.; Lozano, A.; Carrero, S.; Nieto, J. M.; Pérez-  
583 López, R.; Fernández-Martínez, A.; Castillo-Michel, H. Recovery of Rare Earth  
584 Elements and Yttrium from Passive-Remediation Systems of Acid Mine Drainage.  
585 *Environ. Sci. Technol.* **2016**, *50*, 8255–8262. DOI: 10.1021/acs.est.6b02084.
- 586 (14) Schaeffer, N.; Passos, H.; Billard, I.; Papaiconomou, N.; Coutinho, J. A. P.  
587 Recovery of Metals from Waste Electrical and Electronic Equipment (WEEE)  
588 Using Unconventional Solvents Based on Ionic Liquids. *Crit. Rev. Environ. Sci.*  
589 *Technol.* **2018**, *4*, 859–922. DOI: 10.1080/10643389.2018.1477417.
- 590 (15) Freire, M. G.; Cláudio, A. F. M.; Araújo, J. M. M.; Coutinho, J. A. P.; Marrucho,  
591 I. M.; Lopes, J. N. C.; Rebelo, L. P. N. Aqueous Biphasic Systems: A Boost  
592 Brought about by Using Ionic Liquids. *Chem. Soc. Rev.* **2012**, *41*, 4966–4995.  
593 DOI: 10.1039/c2cs35151j.
- 594 (16) *Partitioning in Aqueous Two-Phase System*; Walter, H., Brooks, D. E., Fisher, D.,  
595 Eds.; Academic Press, 1985. DOI: 10.1016/B978-0-12-733860-6.50006-2.
- 596 (17) Albertsson, P. Å. *Partition of Cell Particles and Macromolecules*, 2nd ed.; John  
597 Wiley & Sons Inc.: New York, 1971.
- 598 (18) Onghena, B.; Opsomer, T.; Binnemans, K. Separation of Cobalt and Nickel Using  
599 a Thermomorphic Ionic-Liquid-Based Aqueous Biphasic System. *Chem.*  
600 *Commun.* **2015**, *51*, 15932–15935. DOI: 10.1039/c5cc06595j.
- 601 (19) Akama, Y.; Ito, M.; Tanaka, S. Selective Separation of Cadmium from Cobalt,  
602 Copper, Iron (III) and Zinc by Water-Based Two-Phase System of  
603 Tetrabutylammonium Bromide. *Talanta* **2000**, *53*, 645–650. DOI: 10.1016/S0039-  
604 9140(00)00555-5.
- 605 (20) Akama, Y.; Sali, A. Extraction Mechanism of Cr(VI) on the Aqueous Two-Phase  
606 System of Tetrabutylammonium Bromide and (NH<sub>4</sub>)<sub>2</sub>SO<sub>4</sub> Mixture. *Talanta* **2002**,  
607 *57*, 681–686. DOI: 10.1016/S0039-9140(02)00076-0.
- 608 (21) Álvarez-Valero, A. M.; Pérez-López, R.; Matos, J.; Capitán, M. A.; Nieto, J. M.;  
609 Sáez, R.; Delgado, J.; Caraballo, M. Potential Environmental Impact at São  
610 Domingos Mining District (Iberian Pyrite Belt, SW Iberian Peninsula): Evidence  
611 from a Chemical and Mineralogical Characterization. *Environ. Geol.* **2008**, *55*,

- 612 1797–1809. DOI: 10.1007/s00254-007-1131-x.
- 613 (22) Cláudio, A. F. M.; Ferreira, A. M.; Shahriari, S.; Freire, M. G.; Coutinho, J. A. P.  
614 Critical Assessment of the Formation of Ionic-Liquid-Based Aqueous Two-Phase  
615 Systems in Acidic Media. *J. Phys. Chem. B* **2011**, *115*, 11145–11153. DOI:  
616 10.1021/jp204865a.
- 617 (23) Durães, N.; Bobos, I.; da Silva, E. F. Speciation and Precipitation of Heavy Metals  
618 in High-Metal and High-Acid Mine Waters from the Iberian Pyrite Belt (Portugal).  
619 *Environ. Sci. Pollut. Res.* **2017**, *24*, 4562–4576. DOI: 10.1007/s11356-016-8161-  
620 4.
- 621 (24) Costa, M. C.; Duarte, J. C. Bioremediation of Acid Mine Drainage Using Acidic  
622 Soil and Organic Wastes for Promoting Sulphate-Reducing Bacteria Activity on a  
623 Column Reactor. *Water. Air. Soil Pollut.* **2005**, *165*, 325–345. DOI:  
624 10.1007/s11270-005-6914-7.
- 625 (25) Flexer, V.; Baspineiro, C. F.; Galli, C. I. Lithium Recovery from Brines: A Vital  
626 Raw Material for Green Energies with a Potential Environmental Impact in Its  
627 Mining and Processing. *Sci. Total Environ.* **2018**, *639*, 1188–1204. DOI:  
628 10.1016/j.scitotenv.2018.05.223.
- 629 (26) Anraha Bahta; Parker, G. A.; Tuck, D. G. Critical Survey of Stability Constants of  
630 Complexes of Thiocyanate Ion. *Pure Appl. Chem.* **1997**, *69*, 1489–1548. DOI:  
631 10.1351/pac199769071489
- 632 (27) Lommelen, R.; Vander Hoogerstraete, T.; Onghena, B.; Billard, I.; Binnemans, K.  
633 Model for Metal Extraction from Chloride Media with Basic Extractants: A  
634 Coordination Chemistry Approach. *Inorg. Chem.* **2019**, *58*, 12289–12301. DOI:  
635 10.1021/acs.inorgchem.9b01782.
- 636 (28) Shibukawa, M.; Nakayama, N.; Hayashi, T.; Shibuya, D.; Endo, Y.; Kawamura, S.  
637 Extraction Behaviour of Metal Ions in Aqueous Polyethylene Glycol-Sodium  
638 Sulphate Two-Phase Systems in the Presence of Iodide and Thiocyanate Ions.  
639 *Anal. Chim. Acta* **2001**, *427*, 293–300. DOI: 10.1016/S0003-2670(00)01207-1.
- 640 (29) Patrício, P. da R.; Mesquita, M. C.; da Silva, L. H. M.; Da Silva, M. C. H.  
641 Application of Aqueous Two-Phase Systems for the Development of a New  
642 Method of Cobalt(II), Iron(III) and Nickel(II) Extraction: A Green Chemistry  
643 Approach. *J. Hazard. Mater.* **2011**, *193*, 311–318. DOI:  
644 10.1016/j.jhazmat.2011.07.062.
- 645 (30) Rodrigues, G. D.; da Silva, M. do C. H.; da Silva, L. H. M.; Paggioli, F. J.; Minim,

- 646 L. A.; Reis Coimbra, J. S. dos. Liquid-Liquid Extraction of Metal Ions without Use  
647 of Organic Solvent. *Sep. Purif. Technol.* **2008**, *62*, 687–693. DOI:  
648 10.1016/j.seppur.2008.03.032.
- 649 (31) Álvarez, M. S.; Gutiérrez, E.; Rodríguez, A.; Sanromán, M. Á.; Deive, F. J.  
650 Environmentally Benign Sequential Extraction of Heavy Metals from Marine  
651 Sediments. *Ind. Eng. Chem. Res.* **2014**, *53*, 8615–8620. DOI: 10.1021/ie500927q.
- 652 (32) Boudesocque, S.; Mohamadou, A.; Dupont, L.; Martinez, A.; Déchamps, I. Use of  
653 Dicyanamide Ionic Liquids for Extraction of Metal Ions. *RSC Adv.* **2016**, *6*,  
654 107894–107904. DOI: 10.1039/C6RA18991A.
- 655 (33) Diabate, P.; Dupont, L.; Boudesocque, S.; Mohamadou, A. Novel Task Specific  
656 Ionic Liquids to Remove Heavy Metals from Aqueous Effluents. *Metals (Basel)*.  
657 **2018**, *8*, 412. DOI: 10.3390/met8060412.
- 658 (34) Sasic, S.; Zoric, D.; Jeremic, M.; Antic-Jovanovic, A. Study of Complex  
659 Formation in Al(III)-Thiocyanate-Water System via Raman Spectra and Factor  
660 Analysis. *Polyhedron* **2001**, *20*, 839–847. DOI: 10.1016/S0277-5387(01)00699-4.
- 661 (35) Ventura, S. P. M.; Marques, C. S.; Rosatella, A. A.; Afonso, C. A. M.; Gonçalves,  
662 F.; Coutinho, J. A. P. Toxicity Assessment of Various Ionic Liquid Families  
663 towards *Vibrio Fischeri* Marine Bacteria. *Ecotoxicol. Environ. Saf.* **2012**, *76*, 162–  
664 168. DOI: 10.1016/j.ecoenv.2011.10.006.
- 665 (36) Papaiconomou, N.; Vite, G.; Goujon, N.; Lévêque, J. M.; Billard, I. Efficient  
666 Removal of Gold Complexes from Water by Precipitation or Liquid-Liquid  
667 Extraction Using Ionic Liquids. *Green Chem.* **2012**, *14*, 2050–2056. DOI:  
668 10.1039/c2gc35222b.
- 669 (37) Gras, M.; Duclos, L.; Schaeffer, N.; Mogilireddy, V.; Svecova, L.; Eric Chaînet;  
670 Billard, I.; Papaiconomou, N. A Comparison of Cobalt and Platinum Extraction in  
671 Hydrophobic and Hydrophilic Ionic Liquids: Implication for Proton Exchange  
672 Membrane Fuel Cell Recycling. *ACS Sustain. Chem. Eng.* **2020**, *8*, 15865–15874.  
673 DOI: 10.1021/acssuschemeng.0c04263.
- 674 (38) Génand-Pinaz, S.; Papaiconomou, N.; Leveque, J. M. Removal of Platinum from  
675 Water by Precipitation or Liquid-Liquid Extraction and Separation from Gold  
676 Using Ionic Liquids. *Green Chem.* **2013**, *15*, 2493–2501. DOI:  
677 10.1039/c3gc40557e.
- 678

679 **Graphical Abstract**

680



681

682

683 **Synopsis**

684 Development of a tunable system for the sequential selective recovery of transition metals  
685 from acid mine drainage.